UCSF
UC San Francisco Previously Published Works

Title
Thermal constraints on in vivo optogenetic manipulations

Permalink
https://escholarship.org/uc/item/2k08875m

Journal
Nature Neuroscience, 22(7)

ISSN
1097-6256

Authors
Owen, Scott F
Liu, Max H
Kreitzer, Anatol C

Publication Date
2019-07-01

DOI
10.1038/s41593-019-0422-3

Peer reviewed

eScholarship.org Powered by the California Digital Library
University of California

Author Manuscript

Author Manuscript

Author Manuscript

Author Manuscript

HHS Public Access

Author manuscript

Nat Neurosci. Author manuscript; available in PMC 2019 December 17.

Published in final edited form as:

Nat Neurosci. 2019 July ; 22(7): 1061–1065. doi:10.1038/s41593-019-0422-3.

Thermal constraints on *in vivo* optogenetic manipulations

Scott F. Owen[1,7], **Max H. Liu**[2,3,7], and **Anatol C. Kreitzer**[1,4,5,6,8]

[1.]Gladstone Institutes, San Francisco, CA 94158, USA

[2.]Medical Scientist Training Program, University of California, San Francisco, San Francisco, CA 94158, USA.

[3.]Neuroscience Graduate Program, Kavli Institute for Fundamental Neuroscience, UCSF, San Francisco, CA 94158, USA

[4.]Department of Neurology, UCSF, San Francisco, CA 94158, USA

[5.]UCSF Weill Institute for Neurosciences, UCSF, San Francisco, CA 94158, USA

[6.]Department of Physiology, UCSF, San Francisco, CA 94158, USA

[7.]These authors contributed equally to this work

[8.]Lead Contact

Abstract

A key assumption of optogenetics is that light only affects opsin-expressing neurons. However, illumination invariably heats tissue, and many physiological processes are temperature-sensitive. Commonly-used illumination protocols increased temperature by 0.2–2°C and suppressed spiking in multiple brain regions. In striatum, light delivery activated an inwardly-rectifying potassium conductance and biased rotational behavior. Thus, careful consideration of light delivery parameters is required, as even modest intracranial heating can confound interpretation of optogenetic experiments.

Light delivery into living brain tissue is critical for many neuroscience assays, including optogenetic manipulations and fluorescence imaging. These approaches assume that light does not directly affect neuronal physiology. However, experimental measurements and modeling calculations[1,2] describe heating of 0.2–2 °C following sustained illumination of brain tissue with commonly used light powers (3–30 mW). Many neuronal circuit processes are temperature-dependent[3], including ion channel conductance[4] and synaptic transmission[5,6]. Notably, changes in temperature have been used to alter neuronal physiology in rodent cortex[1] and songbird area HVC[7]. In *ex vivo* brain-slice recordings,

Users may view, print, copy, and download text and data-mine the content in such documents, for the purposes of academic research, subject always to the full Conditions of use:http://www.nature.com/authors/editorial_policies/license.html#terms

Correspondence: anatol.kreitzer@gladstone.ucsf.edu.

AUTHOR CONTRIBUTIONS

S.F.O., M.H.L and A.C.K. designed experiments, S.F.O. and M.H.L. performed experiments and analyzed data and all authors wrote the manuscript.

COMPETING INTERESTS

The authors have no competing interests to disclose.

Author Manuscript Author Manuscript Author Manuscript Author Manuscript

illumination-induced heating is reported to generate changes in spiking across various brain regions[8], raising the possibility that temperature changes occurring during *in vivo* optogenetic manipulations could have both electrophysiological and behavioral consequences.

Here we explicitly test this assumption through *ex vivo* recordings in mouse striatum, hippocampus, and cortex, as well as *in vivo* recordings in mouse striatum. Our results indicate that continuous illumination at powers commonly used for optogenetic experiments (10–15 mW) markedly suppresses the firing rates of specific cell types across a range of brain regions, even in the absence of opsin expression. Experiments in medium spiny neurons (MSNs), the principal neurons in the striatum, demonstrate that this light-induced suppression of spiking can be reproduced by direct heating of brain tissue and results from activation of an inwardly-rectifying potassium conductance. Finally, illumination of the striatum in freely moving mice produces a rotational bias, demonstrating that light alone may be sufficient to affect behavior in the absence of opsin expression.

To test how light delivery affects the activity of striatal MSNs *in vivo*, we performed acute single-unit recordings in the dorsal striatum of awake, head-fixed, wild-type mice (Figure 1A,B). Putative MSNs were distinguished from other cell types based on waveform (Figure S1A,B). Despite the lack of opsin or fluorophore expression, light delivery through an optical fiber reversibly suppressed spiking activity in MSNs. This suppression was statistically significant at the population level for both the lower (3 mW) and higher (15 mW) light powers but was most evident at the higher light power (Figure 1C,D, S1C–F).

We considered several explanations for this suppression of activity, including physiological responses to local heating of brain tissue and sensory responses to light detection at the back of the retina. To rule out the latter possibility, we tested whether equivalent physiological responses could be detected in an acute slice preparation. We obtained whole-cell recordings from MSNs in acute slices from wild-type mice using a potassium-based internal solution (Figure 1E). A current injection through the recording pipette elicited spiking in MSNs, which are otherwise quiescent (Figure 1F). In agreement with the *in vivo* results, light delivery through an optical fiber at low power (3 mW) caused a modest drop in firing rate, while higher power (15 mW) reduced spiking more markedly (Figure 1G,H, S1G–I).

To investigate whether this suppression of activity is specific to MSNs, we repeated this experiment in other cell types in the hippocampus and cortex. Spiking activity in CA1 pyramidal neurons was unaffected by light, while dentate gyrus granule cells and cortical layer 5 pyramidal neurons were modestly suppressed (Figure 1I–L, S1J–O). The suppression of cortical pyramidal neurons was surprising with respect to previous reports that light-driven temperature changes increase in cortical activity *in vivo*[1]. To reconcile these results, we recorded from cortical layer 5 fast-spiking interneurons (FSIs), identified by narrow action potential waveforms. The suppression of cortical FSIs was stronger than that of neighboring pyramidal neurons (Figure 1K,L, S1M–O), suggesting that the light-driven elevation of cortical neuron activity reported *in vivo*[1] may arise from disinhibition through suppression of neighboring inhibitory interneurons.

Author Manuscript Author Manuscript Author Manuscript Author Manuscript

We hypothesized these responses to light delivery could arise from local heating of brain tissue. We therefore acutely inserted a miniaturized thermocouple probe in the place of the recording electrode *in vivo*. As predicted by measurement and modeling in other brain regions[1,2], light delivery caused a transient increase in temperature of up to 2 °C (Figure 2A,B, S2A). The time-course of this temperature change, when fit with a single exponential (Figure 2B), matched closely with the decrease in MSN firing (Figure 2C). Temperature changes in the slice were also graded by light power (0.2–1 °C), and closely matched the outward currents measured in MSNs held at −50 mV using a potassium-based internal solution (Figure 2D–G).

To test whether a temperature change was sufficient to elicit this outward current, we established a system to change the temperature in acute slices locally and rapidly using a small copper tube perfused with hot, warm, or cold water (Figure 2H). Measured temperature changes were +1.92 °C (hot), +0.89 °C (warm), or −2.82 °C (cold) (Figure 2I). Whole-cell recordings measured the physiological consequences of this temperature change in MSNs voltage-clamped at −50 mV with a potassium-based internal solution. Warming the slice elicited a graded, outward current with a time-course that tracked the temperature change, while cooling of the slice reduced this outward current (Figure 2J). The relationship between temperature and current was strikingly linear, suggesting temperature-dependent modulation of a tonically-active current (Figure 2K).

To better understand the relationship between light delivery and heating, we used a recently published model[1] to predict the local temperature changes as a function of light power and pulse duration (Figure 2L). This plot includes a “threshold” line at a temperature change of approximately 0.1 °C, which corresponds to the intensity and duration at which we begin to observe physiological effects in wild-type MSNs (Figure 1; 3 mW for 1 sec). High light powers (≥30 mW) cause minimal heating if pulse durations are shorter than 100 ms. However, long periods of continuous light, as are commonly used for optogenetic inhibition, cause significant heating even at modest powers (3–5 mW). This model efficiently describes how changes in duty cycle, pulse frequency, and wavelength affect temperature during single light pulses, and pulse trains (Figures S2D,E and S3).

To characterize the physiology of this light-evoked current, we performed whole-cell voltage-clamp recordings in which we varied the holding potential of MSNs between −140 mV and −50 mV (Figure 2M–O). Consistent with activation of a potassium conductance, the current reversed at −93 mV and showed a striking inward rectification (Figure 2O). This light-induced current was almost entirely abolished in MSNs recorded using a cesium-based internal solution (Figure 2P). Furthermore, in MSNs recorded with a potassium-based internal, the light-induced current was sensitive to bath application of $BaCl_2$ at a concentration of 250 μM (Figure 2Q,R). These results are most consistent with activation of an inwardly-rectifying potassium channel (Figure 2D–R). Together, our data indicate that light delivery in striatum using commonly applied experimental parameters can heat brain tissue sufficiently to alter MSN activity through activation of an inwardly-rectifying potassium conductance in MSNs, leading to the suppression of firing in the absence of opsin expression.

Author Manuscript Author Manuscript Author Manuscript Author Manuscript

In contrast to the brief pulses of high intensity illumination used in optogenetics, imaging experiments often require lower intensity illumination for longer durations, spanning minutes to hours. Cortical heating during high-intensity multiphoton illumination has been described in some detail[9]. Therefore, we explored the temperature changes resulting from long-duration, low-intensity illumination through optical fibers, as occur in fiber photometry experiments. This revealed a modest temperature increase that rapidly reached an intensity-dependent plateau (Figure S2F). These data suggest that illumination for photometry experiments should be maintained at less than 0.25 mW average power to avoid temperature-dependent changes in physiological activity.

Finally, we tested whether this light-driven suppression of MSNs can affect animal behavior (Figure 3, S4). We implanted optical fibers into the dorsal striatum of wild-type mice and delivered light unilaterally, using automated post-hoc tracking to monitor body position. Light delivery reversibly biased rotations in the direction ipsilateral to the illumination, consistent with suppression of striatal network activity (Figure 3, S4). Light-driven, opsin-independent suppression of striatum can therefore affect behavioral as well as physiological results.

The conductance of several potassium channel subtypes is temperature-dependent[4]. Thermo-sensitivity has been suggested for K_{ir} inwardly-rectifying channels based on structural homology to thermoTRP channels[10], and sensitivity to barium or cesium is a primary hallmark of K_{ir} channels (Figure 2J–L). In our recordings, light-mediated suppression of spiking correlates with brain regions that express K_{ir} channels, including dentate gyrus, cortex, and striatum but not the CA1 pyramidal neurons in hippocampus[11]. We therefore suggest that the light-activated potassium current described here most likely arises from temperature-dependent modulation of inwardly-rectifying potassium channels.

Our experiments indicate that light-driven temperature changes can reduce firing rates of many types of neurons, and the magnitude of this effect is sufficient to affect behavior. With this in mind, we suggest two experimental design considerations: minimization of light power and duration, and careful control experiments that account for off-target effects of light delivery[3,12]. These control experiments should consist of (1) opsin-free controls, in which light is delivered but no opsin is present, and (2) light-free controls, in which the opsin is expressed but light is not delivered[12]. Importantly, the efficiency of optical fiber implants, the power and duration of light delivery, and the quality of the surgical preparation must be identical for all control animals. Blinding of the experimenter to the identity of animals during surgical preparation and performance of experiments can help ensure the rigor of these procedures.

Several factors can minimize light delivery while preserving activation of opsins. Excitatory opsins such as channelrhodopsin-2 express well within ~2 weeks of virus injection, whereas inhibitory opsins such as eNpHR3.0 or eArchT can take as long as 6–8 weeks to develop significant photocurrents in response to modest illumination because of limited membrane trafficking[13]. Any apparent physiological responses to light that occur before opsin expression is fully developed should clearly be treated with caution.

Author Manuscript Author Manuscript Author Manuscript Author Manuscript

Careful consideration of the time-course of light-driven responses can help to differentiate opsin-driven effects from opsin-independent experimental artifacts. The time-constants with which optogenetic proteins alter neuronal activity are on the order of ones to tens of milliseconds. This is true for direct optogenetic excitation of neuronal populations[14], and for indirect synaptic disinhibition arising from optogenetic silencing of inhibitory neuronal populations[15,16]. By contrast, the time-constant for heating of neuronal tissue with light is markedly slower[1,2] (Figure 2A–F, S2A–C). Physiological responses that develop slowly, over hundreds of milliseconds or seconds should therefore be suspected of arising from local heating of tissue rather than a direct opsin-dependent physiological process. In these cases, we suggest that a higher bar ought to be met by the experimenter to describe a mechanism to reconcile the time-course of the optogenetic manipulation with the time-course of the physiological response and to establish the rigor of opsin-independent control experiments. The continuously growing toolbox of opsins with altered spectral sensitivity[17] or kinetics[18] opens the door for use of lower light powers or longer wavelengths that generate less heating (Figure S2E). New technologies, including tapered fibers, waveguides, and micro-LEDs that spread light more evenly across the tissue, also support more efficient and homogenous opsin activation across larger brain structures[19,20], which should help mitigate artifacts arising from tissue heating.

METHODS

Experimental model and subject details

52 adult mice on a C57BL/6 background, aged 45 to 250 days, of both sexes were used in experiments. All animals were group housed and maintained on a 12/12 light dark cycle and fed ad libitum. N=3 wild-type mice (2 female; 1 male; Jackson Stock #000664) were used for *in vivo* electrophysiology experiments. N=4 wild-type mice (2 female; 2 male; Jackson Stock #000664) were used for *in vivo* temperature recording experiments. N=29 wild-type mice (12 males; 17 females; Jackson Stock #000664) were used in slice electrophysiology experiments. N=5 PV-2A-cre mice (5 female; Jackson Stock #012358) were used for *in vivo* optogenetic suppression of FSIs. N=11 wild-type mice (4 female; 7 male; Jackson Stock #000664) were used for open-field behavioral experiment.

Sample size for physiological recordings were determined based on previously published studies[1,13,14,16], and statistical significance was calculated using post hoc tests. Recordings were performed in a standardized way to minimize possibility for experimenter bias. Age and sex of mice was balanced across cohorts, and littermates were used for fluorophore control experiments.

Stereotactic surgery

All procedures were in accordance with protocols approved by the UCSF Institutional Animal Care and Use Committee. Experiments were carried out during the light cycle. All surgeries were carried out under aseptic conditions, while mice were anaesthetized with isoflurane (3% for induction, 0.5–1.5% for maintenance) in a manual stereotactic frame (Kopf). Buprenorphine HCl (0.1 mg/kg, intraperitoneal injection) and Ketoprofen (5mg/kg, subcutaneous injection), were used for postoperative analgesia.

Author Manuscript Author Manuscript Author Manuscript Author Manuscript

Headbar implantation.

WT mice were prepared for *in vivo* awake head-fixed recordings by surgical implantation of a headbar. Animals were mounted onto the stereotax and anaesthesia was induced as described above. The overlying scalp was removed, and the skull was cleaned and exposed. A stainless steel headbar (eMachineShops, custom design) was then secured with a combination of dental adhesives (C&B Metabond, Parkell, Lang). After dental adhesive had set, mice were allowed to recover for at least 7 days before head fixation or recordings.

Head-fixed *in vivo* electrophysiology recordings

At least three days prior to recording, animals were acclimated to a head fixation device, consisting of a custom 3-D printed cylindrical running wheel (custom design, Evan Feinberg). The night before a recording session, animals were anesthetized and mounted on a stereotax as described above. Craniectomies were made above the targeted recording area in dorsal striatum (+1.0 AP, +/−2.0 ML) bilaterally and covered with silicone elastomer (Body Double). Animals were then allowed to recover overnight before recording.

Extracellular recordings were performed using the Trodes data acquisition system (Spike Gadgets Trodes 1.7.3), and a 32 channel silicon probe (Cambridge Neurotech, ASSY-37 DBC-2–2, 2 shank probe with parallel electrodes, 9 mm length, 250 μm inter-shank spacing, 16 sites per shank). A 200 μm, 0.39 NA optical fiber was attached for light delivery (Thorlabs FT200UMT, flat cut, mounted 750 μm above electrode sites, tip centered between shanks). Laser light was generated by TTL control of a 532 nm DPSS laser (Shanghai Laser Co). Previously published data[16] in Figure S2C were acquired using a combination of Trodes and Plexon (version 2.6) acquisition systems.

Animals were head-fixed and the craniectomy exposed. Masking lights, consisting of two green LEDs (Sparkfun COM-00105) were positioned bilaterally 2 cm lateral to the head and illuminated throughout the experiment. A bank of 36 white LEDs (Sparkfun COM-0053) was positioned 15 cm anterior and superior to the mouse head and illuminated throughout the experiment. Finally, aluminum blinding dividers were along the side of the head to reduce the visual stimulation by the light stimulation. The probe was then coated with CM-DiI to facilitate post-hoc reconstruction of the electrode track (ThermoFisher V22888), and lowered through the craniectomy under the control of a motorized micromanipulator (Siskiyou MX1641L) until electrodes were in striatum (minimum depth of 2 mm from brain surface). The probe was allowed to settle for at least 30 minutes before recording. The recording sites centered on the dorsal striatum at +1.0 AP, +/−2.0 ML, −2.5 DV from brain surface

Recordings were sampled at 30 kHz, band-pass filtered (300–6,000 Hz), and analyzed for spiking activity. Single units were isolated manually using peak amplitude and principal components as variables, using the MatClust script (SpikeGadgets). Electrode tracts were reconstructed post hoc using DiI fluorescence to confirm recording location.

Light power was measured at the fiber tip before and after recordings (Thorlabs PM-100D with S130C). Animals received 5 seconds of light at either 3 mW or 15 mW per trial, with a

Author Manuscript Author Manuscript Author Manuscript Author Manuscript

15 second inter-stimulation interval. Light power was varied in two sets of interleaved 50 trial blocks.

Head-fixed *in vivo* temperature measurement

WT animals were prepared with headbar surgery as described above, with the addition of a 200 μm, 0.39 NA optical fiber (Thorlabs FT200UMT, flat cut) chronically implanted into the brain and affixed to the skull during headbar surgery. The optical fiber was implanted at −1.0 AP, 2.0 ML, −3.0 DV and angled at 30 degrees from vertical in the posterior direction, to ensure ~1 mm of distance between the fiber tip and the thermocouple. Craniectomy sites were the same as for recordings.

Mice were allowed to recover for two weeks then acclimated to head fixation as described above. Following acclimation, a craniectomy was made over marked sites and animals were recorded from the following day. Temperature recordings were performed with an OMEGA DAQ acquisition system (model 2401) coupled to a T-type hypodermic thermocouple (MT 29/5, Physitemp) using OMEGA DAQ CENTRAL software 1.0.7. The thermocouple was coated in CM DiI (Thermofisher) to mark the tract and inserted acutely using a micromanipulator. After allowing temperature to stabilize, temperature change in response to laser illumination was recorded. Each laser power was delivered 30 times, with 5 second pulse duration and 20 second interval between onset of laser pulses.

Acute slice physiology

Wild-type mice 8–24 weeks of age were euthanized with a lethal dose of ketamine and xylazine followed by transcardial perfusion with 8 mL of ice cold artificial corticospinal fluid (ACSF) containing (in mM): NaCl (79), KCl (2.3), $NaHCO_3$ (23), Sucrose (68), NaH_2PO_4 (1.1), $MgCl_2$ (6), D-Glucose (12), $CaCl_2$ (0.5). Coronal slices (250 μm thick) containing dorsal striatum, primary sensory cortex, or dorsal hippocampus were then prepared with a vibratome (Leica) in the same solution before incubation in 33°C ACSF containing (in mM): NaCl (125), $NaHCO_3$ (26), NaH_2PO_4 (1.25), KCl (2.5), $MgCl_2$ (1), $CaCl_2$ (2), and D-Glucose (12.5), continuously bubbled with 95/5% O_2/CO_2. After 30–60 minutes of recovery at 35 °C, slices were kept at room temperature until recording. For recordings, slices were transferred to a chamber superfused with recording ACSF (4–6 mL min^{-1}) at 28 °C.

Whole-cell current-clamp recordings were obtained with an internal solution containing (in mM): K-Gluconate (135), NaCl (10), $MgCl_2$ (2), EGTA (0.5), HEPES (10), Mg-ATP (2), Na-GTP (0.3). Physiological activity was recorded using Igor Pro (version 6.0). Spiking activity was driven by injection of current steps 3 sec in duration through the recording pipette with an inter-sweep interval of 10–60 sec. Injection amplitude was chosen to drive spiking that was maintained throughout the 3 sec current step (250–600 pA). On interleaved sweeps, green laser light (532 nm) was delivered through a 200 μm optical fiber placed 500–800 μm from the recorded neuron at a power of either 3 mW or 15 mW. Light pulses were 1 sec in duration, spanning the middle 1 sec of the 3 sec current step injection. To calculate group data for spike rate modulation by light, the spike rate for each neuron on Light On trials was normalized to the spike rate for the equivalent period on Light Off trials. Three

Author Manuscript Author Manuscript Author Manuscript Author Manuscript

separate periods were analyzed, “Pre” (0–1 sec), “Light” (1–2 sec), and “Post” (2–3 sec after start of current step). To identify cortical neuron cell types, each waveform was up-sampled 10-fold using a spline fitting function in MATLAB (version 2014a), before calculating an average spike waveform from that neuron. The spike width was calculated as the full-width-half-maximum value of the action potential peak relative to the pre-spike baseline membrane potential. A clear bimodal distribution emerged to distinguish putative pyramidal neurons (width > 0.7 ms) from putative interneurons (width < 0.7 ms).

Whole-cell voltage-clamp recordings of light-activated currents were performed using the same potassium-based internal solution in a set of neurons that partially overlapped with the current-clamp recordings. For whole-cell voltage-clamp recordings with a cesium-based internal solution, the internal recording solution contained (in mM): $CsMeSO_3$ (135), NaCl (8), EGTA (0.5), HEPES (10), Mg-ATP (2), Na-GTP (0.3), and QX-314 (5). For all voltage-clamp recordings, MSNs were held at a resting potential of −85 mV between sweeps. Membrane potentials are not corrected for junction potential. On each sweep, the voltage was stepped to −50 mV for 3 sec, and the light pulse (1 sec in duration) was delivered for the middle 1 sec of the 3 sec voltage step. Inter-sweep interval was 10–20 sec. Current amplitude was measured across three separate time windows: “Pre” (0.75–1 sec), “Light” (1.75–2 sec), and “Post” (2.5–2.75 sec after start of voltage step). The light-induced current was calculated by subtracting the average current amplitude over the “Pre” and “Post” periods from the average current over the “Light” period. This average was calculated separately for “Light On” and “Light Off” sweeps, and the final light-induced current for each cell was determined by subtracting the “Light Off” value from the “Light On” value.

An equivalent protocol was used to calculate the I-V curve and rectification of the light-activated current. The MSN was held at a resting potential of −85 mV with a potassium-based internal recording solution, and the voltage was stepped to varying holding potentials over a range from −140 mV to −50 mV for 3 sec with the light pulse (1 sec in duration) delivered over the middle 1 sec of the 3 sec voltage step.

For $BaCl_2$ wash-in experiments, the inter-sweep interval was extended to 60 sec. Light-activated currents were recorded at a holding potential stepped to −50 mV with a potassium-based internal as described above. Recordings were maintained for at least 5 minutes after break-in to ensure recording stability before introducing 250 μM $BaCl_2$ to the bath solution. Recordings were maintained for at least 15–20 min following the application of $BaCl_2$. Leak current was measured as the average current over 250 ms before onset of the light, and was subtracted from each trace to account for effects of $BaCl_2$ on leak or background conductance independent of its effect on the light-activated current.

Temperature control in acute slices

A custom-designed system was constructed to locally control temperature in acute slices. A short length of copper tubing was bent into a U-shape, and an additional copper extension was soldered to the end of the U to contact the slice. A peristaltic pump produced a recirculating flow while solenoids were used to gate the source of temperature-controlled water inside the copper tubing. Controlled warming of the tubing was accomplished by rapidly switching the flow from an in-line solution heater (Warner Instruments) to pass

Author Manuscript Author Manuscript Author Manuscript Author Manuscript

through the copper tubing using TTL-gated solenoids (NResearch) to rapidly switch fluid flow. Cooling was accomplished by rapidly switching the flow to a source that passed through a short ~15 cm length of coiled copper tubing inside an ice bath immediately prior to entering the tubing that was in contact with the slice.

Optogenetic silencing of FSIs *in vivo*

Data in Figure S2C were re-analyzed from a previous publication[16] to calculate the time-course of optogenetic responses using z-scored firing rates. To record single unit electrophysiological activity from medium spiny neurons and fast-spiking interneurons *in vivo* during optogenetic silencing of FSIs in awake, freely moving mice, we implanted multi-electrode arrays into striatum of PV-2A-cre mice. Under anesthesia in a stereotactic surgery, the scalp was opened and a hole was drilled in the skull (+0.5 to +1.5 mm AP, −2.5 to −1.5 mm ML from bregma). We injected 1000 nL of AAV (AAV5-EF1α-DIO-eNpHR3.0-YFP) the coordinates +1.0 AP, +/−2.2 ML, −2.5 DV from bregma in PV-2A-cre mice (Jackson Stock #012358). Two skull screws were implanted in the opposing hemisphere to secure the implant to the skull. Dental adhesive (C&B Metabond, Parkell) was used to fix the skull screws in place and coat the surface of the skull. An array of 32 microwires (4×8 array, 35 μm tungsten wires, 150 μm spacing between wires, 150 – 200 μm spacing between rows; Innovative Physiology) was combined with a 200 μm diameter optical fiber (Thorlabs FT200UMT, flat cut) and lowered into the striatum (2.5 mm below the surface of the brain) and cemented in place with dental acrylic (Ortho-Jet, Lang Dental). After the cement dried, the scalp was sutured shut. Animals were allowed to recover for at least seven days before striatal recordings were made.

Voltage signals from each site on a 32-channel microwire array were recorded in awake, freely moving mice in an open field arena. Signals were band-pass-filtered, such that activity between 300 and 6,000 Hz was analyzed as spiking activity. This data was amplified, processed and digitally captured using commercial hardware and software (Plexon or SpikeGadgets). Single units were discriminated with principal component analysis (Plexon Offline Sorter, or SpikeGadgets MatClust). Two criteria were used to ensure quality of recorded units: (1) recorded units smaller than 100 μV (~3 times the noise band) were excluded from further analysis and (2) recorded units in which more than 1% of interspike intervals were shorter than 2 ms were excluded from further analysis. FSIs and MSNs were distinguished based on waveform and firing rate as previously described[16]. Green light pulses 1 sec in duration and 3 mW in brightness were delivered through a 200 μm optical fiber contained within the implanted microwire recording array with a duty cycle of 25% for 60 min (900 pulses for 1 s; 30 pulses for 30 s).

Temperature calibration

Temperature measurements in slice were performed with the same temperature setup of an Omega DAQ box and T-type thermocouple. In the slice rig, the tip of the sensor was placed at the approximate location of the recording site relative to the fiber or copper tubing with the bath perfusion system operating as usual for acute slice recordings. Temperature change was measured during laser delivery or passage of hot, warm, or cold fluids through the copper tubing. Measurements for each power were repeated 30 times.

Author Manuscript Author Manuscript Author Manuscript Author Manuscript

Open Field Behavior

WT animals were prepared with headbar surgery as described above, with the addition of bilateral 200 μm, 0.39 NA optical fibers (Thorlabs FT200UMT, flat cut) chronically implanted into the brain and affixed to the skull during headbar surgery. The optical fibers were implanted at Bregma +1.0 AP, 1.5 ML, −2.2 DV.

Mice were allowed to recover for two weeks then acclimated to human handling. The open field arena was a pair of 25 cm diameter circular arenas lit from below and the sides with bright white LED strip lighting, to minimize the visual salience of laser illumination. Video was recorded at 30 fps using an area scan camera (Basler acA1300–60gm). Laser illumination was generated via two 532 nm DPSS lasers (Shanghai Laser Co), and coupled to commutators (Doric FRJ_1×2i_FC-2FC). Power was tested at the end of the fiber patch cable at the beginning of each behavioral session, and between animals, and was corrected for the recorded efficiency of the implanted fibers for each animal. Mice were run two at a time, one in each behavioral arena.

Fifteen minutes before each behavioral session, animals received an IP injection of 3 mg/kg of amphetamine (d-amphetamine hemisulfate salt, Sigma-Aldrich A5880 in sterile saline). This limited habituation to the open field environment and ensured consistent locomotion throughout behavioral sessions (Figure 3, S4). At the start of each session, a fiber optic patch cable was attached unilaterally to one of the implanted optical fibers in dorsal striatum. The mouse was placed in the open field for 30 minutes, during which time the laser was illuminated in a 10 second on, 30 second off cycle. The optical fiber was then moved to the opposite hemisphere and the behavior was repeated before returning the mouse to its home cage. Laser power was held constant for all sessions on each day. Laser powers were 3 mW (continuous), 7 mW (continuous), 15 mW (continuous), or 15 mW at 20 Hz (15 mW peak power, 10 ms pulse duration for 20% duty cycle). Predicted temperature rises based on previously published computer model[1] for 532 nm light 200 μm below the tip of 200 μm fiber. Continuous video was acquired using a camera mounted above the arena, and was processed post-hoc using DeepLabCut[21].

Data analysis for *in vivo* physiology

Putative medium spiny neurons (MSNs) were identified based on waveform and regularity of firing (minimum ISI coefficient of variation = 1.1, minimum peak-trough spike width = 0.5 ms).

Modulation index was calculated as:

$$\text{Modulation index} = (R1 - R2)/(R1 + R2)$$

R1 represents average firing rate during the entire duration of laser illumination. R2 represents the average firing rate for an equal period of time immediately before laser illumination.

Author Manuscript Author Manuscript Author Manuscript Author Manuscript

Data analysis for open field behavior

Open field videos were first split into individual videos of each area using FFMPEG. Following this, they were processed using DeepLabCut, a machine learning package that can perform tracking of animal features[21]. Data in this paper was analyzed using a network trained on 200 frames of recorded behavior run for 1 million training iterations. The network was trained to detect the tip of the nose, the base of each ear, and the base of the tail. We then extracted the mean position of the two ears by averaging the x and y coordinates of the ears, which we used as the center point of the mouse.

In order to determine total locomotion, we detected the change in position of the central point of the mouse across the entire session, and summed it by session. In order to determine change in mouse speed at laser onset, we extracted speed traces of the mouse center point aligned to laser onset. To determine the direction of the mouse, we generated a vector from the tail base to the center point. We then calculated the change in the direction of the mouse for every laser trial. To determine the rotations of the mouse, we wrote custom MATLAB code (MATHWORKS) that counted 90 degree rotations whenever a mouse changed its direction in one direction for 90 degrees. If the animal turned in the other direction for more than 45 degrees, then rotation tracking was reset for the new direction. Rotation times were defined as the frame in which the animal completed 90 degrees of rotation. Rotational analysis was performed blinded to the side of laser illumination. From these rotations, we then calculated rotational bias in ipsilateral or contralateral direction during the analysis time periods by the formula:

$$\text{Rotational Bias} = (\text{CR} - \text{IR})/(\text{CR} + \text{IR})$$

CR represents contralateral rotations, IR represents ipsilateral rotations.

QUANTIFICATION AND STATISTICAL ANALYSIS

All statistical analyses were performed using standard MATLAB functions or custom MATLAB scripts. Statistical tests used, and P-values are reported in figure legends and results section. Only non-parametric tests that did not include an assumption of distribution normality were used for data analysis. Two-sided signed-rank tests were used for paired data, while two-sided rank-sum tests were used for unpaired data. No statistical methods were used to pre-determine sample sizes but our sample sizes are similar to those reported in previous publications[1,13,14,16]. For acute slice recordings, recordings conditions were not randomized. Within individual whole cell recordings, light-on and light-off trials were interleaved. For comparisons across cells, sham and drug-treatment recordings were counterbalanced within days, as were recordings at different temperature conditions. For *in vivo* recordings, high and low light powers were interleaved in blocks of 50 trials, and all mice were given the same laser light condition during the same day. Light conditions were randomized across days. With the exception of rotational analysis, data collection and analysis were not performed blind to the conditions of the experiments. All slice physiology was analyzed using automated scripts to minimize experimenter bias. No animals were excluded from analysis. Whole-cell recordings with unstable baseline, inadequate access

Author Manuscript Author Manuscript Author Manuscript Author Manuscript

resistance (>20 MOhms), or excessive leak current (>200 pA) were determined to be unhealthy and excluded from analysis. Please refer to the Life Sciences Reporting Summary for additional information.

DATA AND SOFTWARE AVAILABILITY

The data that support the findings of this study are available from the corresponding author upon request. Modeling is based on previously published code that is freely available[1], all other analysis code is available upon request.

Supplementary Material

Refer to Web version on PubMed Central for supplementary material.

ACKNOWLEDGEMENTS

We thank Benjamin Margolin for assistance with genotyping, histology, and microscopy, and the A.C.K. laboratory for comments on the manuscript. This work was funded by NIH R01 NS078435 and RF1 AG047655 (to A.C.K.), NARSAD Young Investigator Award (to S.F.O.), F32 NS083369 (to S.F.O.) and K99 MH110597 (to S.F.O.), and RR018928 (to the Gladstone Institutes)

REFERENCES

1. Stujenske JM, Spellman T & Gordon JA Modeling the Spatiotemporal Dynamics of Light and Heat Propagation for In Vivo Optogenetics. Cell Rep. 12, 525–534 (2015). [PubMed: 26166563]
2. Arias-Gil G, Ohl FW, Takagaki K & Lippert MT Measurement, modeling, and prediction of temperature rise due to optogenetic brain stimulation. Neurophotonics 3, 045007 (2016). [PubMed: 27981063]
3. Yizhar O, Fenno LE, Davidson TJ, Mogri M & Deisseroth K Optogenetics in Neural Systems. Neuron 71, 9–34 (2011). [PubMed: 21745635]
4. Yang F & Zheng J High temperature sensitivity is intrinsic to voltage-gated potassium channels. 15
5. Moser E, Mathiesen I & Andersen P Association between brain temperature and dentate field potentials in exploring and swimming rats. Science 259, 1324–1326 (1993). [PubMed: 8446900]
6. Sabatini BL & Regehr WG Timing of neurotransmission at fast synapses in the mammalian brain. Nature 384, 170–172 (1996). [PubMed: 8906792]
7. Long MA & Fee MS Using temperature to analyse temporal dynamics in the songbird motor pathway. Nature 456, 189–194 (2008). [PubMed: 19005546]
8. Ait Ouares K, Beurrier C, Canepari M, Laverne G & Kuczewski N Opto nongenetics inhibition of neuronal firing. Eur. J. Neurosci 49, 6–26 (2019). [PubMed: 30387216]
9. Podgorski K & Ranganathan G Brain heating induced by near-infrared lasers during multiphoton microscopy. J. Neurophysiol 116, 1012–1023 (2016). [PubMed: 27281749]
10. Yang F, Cui Y, Wang K & Zheng J Thermosensitive TRP channel pore turret is part of the temperature activation pathway. Proc. Natl. Acad. Sci 107, 7083–7088 (2010). [PubMed: 20351268]
11. Prüss H, Derst C, Lommel R & Veh RW Differential distribution of individual subunits of strongly inwardly rectifying potassium channels (Kir2 family) in rat brain. Brain Res. Mol. Brain Res 139, 63–79 (2005). [PubMed: 15936845]
12. Allen BD, Singer AC & Boyden ES Principles of designing interpretable optogenetic behavior experiments. Learn. Mem. Cold Spring Harb. N 22, 232–238 (2015).
13. Gradinaru V et al. Molecular and Cellular Approaches for Diversifying and Extending Optogenetics. Cell 141, 154–165 (2010). [PubMed: 20303157]

Author Manuscript Author Manuscript Author Manuscript Author Manuscript

14. Pi H-J et al. Cortical interneurons that specialize in disinhibitory control. Nature 503, 521–524 (2013). [PubMed: 24097352]
15. Mattis J et al. Principles for applying optogenetic tools derived from direct comparative analysis of microbial opsins. Nat. Methods 9, 159–172 (2012).
16. Owen SF, Berke JD & Kreitzer AC Fast-Spiking Interneurons Supply Feedforward Control of Bursting, Calcium, and Plasticity for Efficient Learning. Cell 172, 683–695.e15 (2018). [PubMed: 29425490]
17. Lin JY, Knutsen PM, Muller A, Kleinfeld D & Tsien RY ReaChR: A red-shifted variant of channelrhodopsin enables deep transcranial optogenetic excitation. Nat. Neurosci 16, 1499–1508 (2013). [PubMed: 23995068]
18. Berndt A, Yizhar O, Gunaydin LA, Hegemann P & Deisseroth K Bi-stable neural state switches. Nat. Neurosci 12, 229–234 (2009). [PubMed: 19079251]
19. Pisanello F et al. Dynamic illumination of spatially restricted or large brain volumes via a single tapered optical fiber. Nat. Neurosci 20, 1180–1188 (2017). [PubMed: 28628101]
20. Steude A, Witts EC, Miles GB & Gather MC Arrays of microscopic organic LEDs for high-resolution optogenetics. Sci. Adv 2, e1600061 (2016). [PubMed: 27386540]

METHODS REFERENCES

21. Mathis A et al. DeepLabCut: markerless pose estimation of user-defined body parts with deep learning. Nat. Neurosci 21, 1281 (2018). [PubMed: 30127430]

Author Manuscript Author Manuscript Author Manuscript Author Manuscript

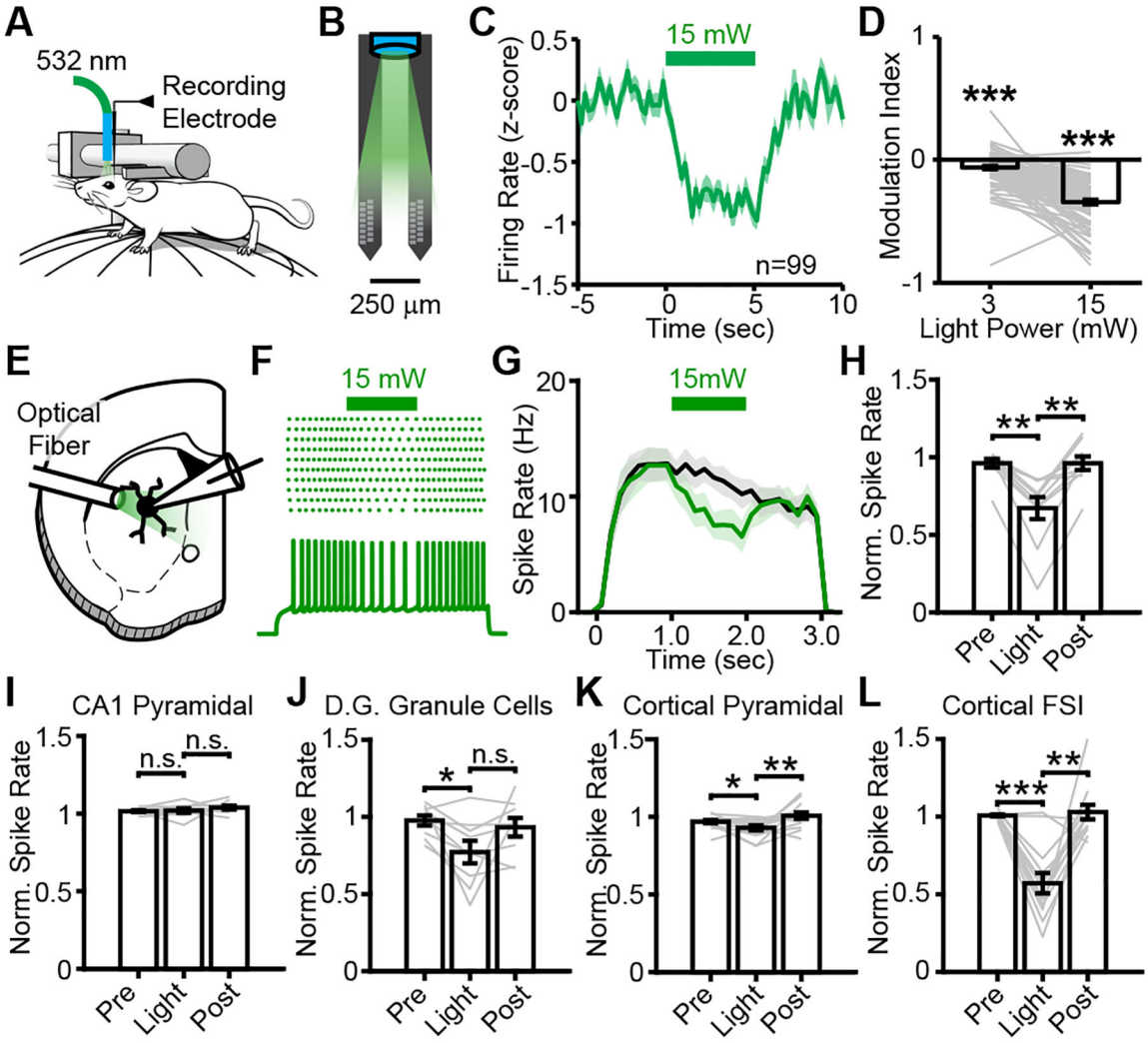

Figure 1. Light delivery suppresses MSN activity *in vivo* and in acute slices.

A,B, Recording and electrode configuration for acute, *in vivo*, head-fixed recordings from awake mice. C,D Mean peri-stimulus aligned firing rate of MSNs in response to 15 mW of 532 nm light and corresponding population average of modulation index. Two-sided signed rank test to compare each distribution against zero. (N=3 mice, n=99 MSNs; $P=6.57\times10^{-7}$ for 3 mW, $P=6.84\times10^{-18}$ for 15 mW). E, Configuration for acute slice whole-cell recordings. F, Exemplar current-clamp recording with spiking elicited by current injection. Light delivered at 15 mW, 532 nm through an optical fiber. G,H, Mean suppression of spiking by light delivery for light on (green) or light off (black) traces. Two-sided signed-rank test. (N=2 mice, n=11 cells; P=0.002 and P=0.010). I-L, Firing rates for CA1 pyramidal neurons (N=6 mice, n=10 cells; P=0.375 and P=0.432), DG Granule cells (N=5 mice, n=9 cells; P=0.012 and P=0.098), cortical L5 pyramidal neurons (N=5 mice, n=15 cells; P=0.026 and P=0.008), and cortical L5 fast-spiking interneurons (N=8 mice, n=13 cells; P=0.001 and P=0.001) in response to light delivery at 15 mW, 532 nm. All tests are two-sided signed-rank tests. * P<0.05, ** P<0.01, *** P<0.001. All error bars and shaded regions represent s.e.m.

Author Manuscript Author Manuscript Author Manuscript Author Manuscript

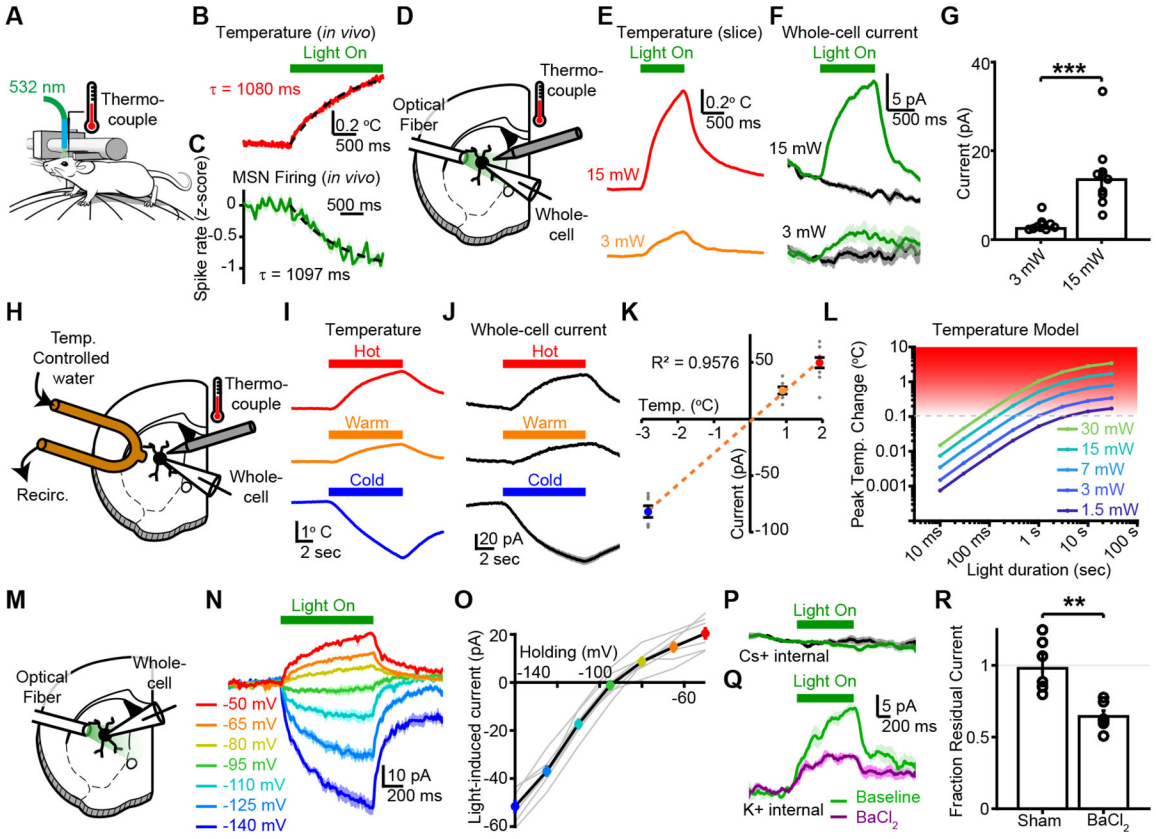

Figure 2. Light-induced heating increases an inwardly-rectifying potassium conductance in MSNs.

A, Configuration for *in vivo* head-fixed temperature measurements and physiology. B, Temperature increase *in vivo* fit to a single exponential (dashed line) (N=1 mouse). C, Time-course of decrease in mean MSN firing rate fit to a single exponential (dashed line). Same data as Figure 1C (N=3 mice, n=99 MSNs). D, Configuration for whole-cell recordings or temperature measurements in acute slices. E, Exemplar temperature change and F, average whole-cell current in exemplar MSN held at −50 mV with potassium-based internal. Light delivery at 3 mW or 15 mW, 532 nm. G, Group data for light-evoked current in MSNs (N=2 mice, n=9 cells for 3mW; N=2 mice, n=10 cells for 15 mW; two-sided rank sum test, $P=4.33\times10^{-5}$). H, Configuration for whole-cell recordings with temperature modulation. I, Temperature changes and J, exemplar whole-cell currents in wild-type MSNs, recorded in voltage-clamp with potassium-based internal. K, Linear relationship between temperature change and current (N=2 mice, n=7 cells for −2.82 °C; N=2 mice, n=7 cells for +0.89 °C; N=2 mice, n=10 cells for +1.92 °C). L, Modeled temperature changes predicted for this recording configuration[1]. M, Recording configuration, N, exemplar traces, and O, group data for voltage sensitivity of light-activated currents (N=2 mice; n=8 cells). P, Exemplar light-activated current recorded at −50 mV with cesium-based internal. Light off (black), light on (green). (N=2 mice, n=10 cells). Q, Exemplar light-activated current recorded at −50 mV with potassium-based internal before (green) and after (purple) bath application of 250 μM $BaCl_2$. R, Group data for $BaCl_2$ sensitivity of light-activated conductance (N=2 mice, n=7

cells sham; N=2 mice, n=6 cells $BaCl_2$, two-sided rank sum test, P=0.001). Error bars and shaded regions are s.e.m. ** P<0.01, *** P<0.001.

Author Manuscript Author Manuscript Author Manuscript Author Manuscript

Author Manuscript Author Manuscript Author Manuscript Author Manuscript

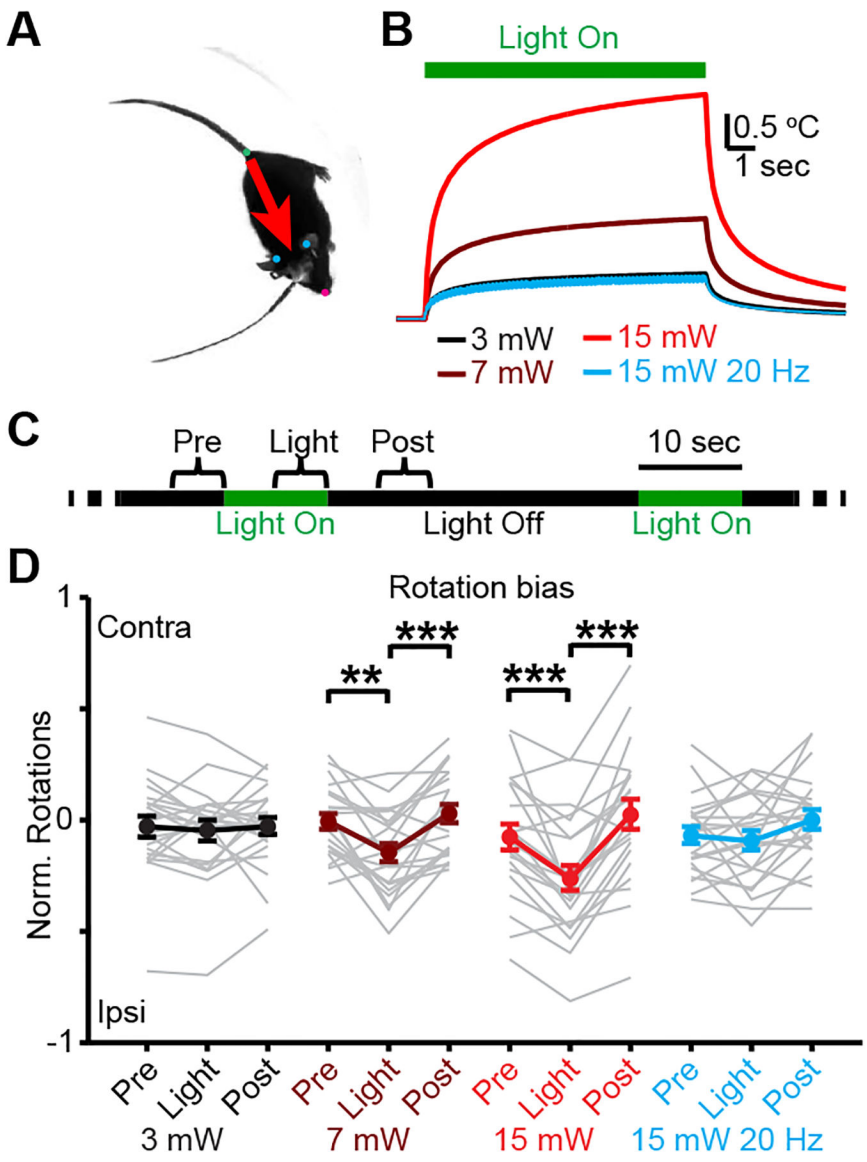

Figure 3: Light delivery in dorsal striatum drives rotational behavior.

A. Video frame illustrating body position tracking. B, Modeled temperature change[1] for continuous or pulsed light delivery at 532 nm. Duty cycle was 20% for pulsed light. C, Light delivery protocol for open field behavioral tests. D, Mean rotational bias in response to light delivery. Two-sided signed-rank test (N=11 mice, 2 hemispheres per mouse, n=22 sessions per condition; 3 mW, P=0.37 and P=0.66; 7 mW, $P=2.7\times10^{-3}$ and $P=3.9\times10^{-4}$; 15 mW, $P=2.3\times10^{-4}$ and $P=1.1\times10^{-5}$; 15 mW at 20 Hz, P=0.94 and P=0.06). ** P<0.01, *** P<0.001. Error bars and shaded regions are s.e.m.